Letter

Emergence of nonequilibrium Lieb excitations in periodically driven strongly interacting bosons

Hoshu Hiyane [1,*] Giedrius Žlabys [1] Thomas Busch [1] and Shohei Watabe [2]

[1] *Quantum Systems Unit, Okinawa Institute of Science and Technology Graduate University, Onna, Okinawa 904-0495, Japan*

[2] *College of Engineering, Shibaura Institute of Technology, 3-7-5 Toyosu, Koto-ku, Tokyo 135-8548, Japan*

(Received 26 December 2024; revised 2 August 2026; accepted 10 October 2026; published 16 November 2026)

The time-averaged spectral function plays a central role in studying the Floquet properties of the many-body fermionic systems. Here, we study the time-averaged spectral function of the periodically driven bosonic systems by providing an exact and rigorous analysis in the strongly interacting one-dimensional limit. The exact analysis reveals that the nonequilibrium Lieb excitations emerge if the underlying steady states form a Floquet-Fermi sea. In the low-frequency limit, we find characteristic linear Lieb excitations that hybridize with Floquet-replica states in the second Floquet-Brillouin zone.

DOI: 10.1103/crbp-vdff

Introduction. Controlling nonequilibrium states in quantum many-body systems offers a promising route for designing novel artificial quantum materials with properties unattainable in equilibrium. A celebrated example is Floquet engineering, which exposes the system to periodic driving [1–4]. Such periodic drives can, for instance, induce artificial magnetic fields in neutral atoms [5–10] or enable the trapping of ions, providing a unique platform for quantum computing [11–14]. These successes of single particle-based Floquet engineering have inspired the exploration of more complex many-body Floquet systems [3,15,16], where Floquet eigenstates and quasienergies play a crucial role. They provide a comprehensive description of the system dynamics analogous to eigenstates and eigenenergies in equilibrium systems [1,17,18], allowing the investigation of the nonequilibrium properties rigorously.

Until recently, measuring the quasienergy spectrum of electrons in a solid was a formidable task, as it required capturing the ultrafast dynamics of the electrons. However, significant development has been made in generating and controlling the femtosecond laser pulse, which led to the realization of the time-resolved angle-resolved photoemission spectroscopy [19–21]. This technique allows one to measure the time-averaged spectral function, which informs the quasienergy weighted by the occupation in the Floquet states. This achievement has opened an era of the Floquet engineering of the electrons in solids. Rapid progress has been made in many-body Floquet physics in solids [19–31], which has stimulated investigations into ultracold fermions [32–37].

In equilibrium bosonic systems, the excitation spectrum is a key quantity of many-body physics, providing direct insight into Bogoliubov quasiparticles [38–43], dynamical instabilities [44–46], roton excitations in supersolid condensates [47–49], and many other collective phenomena [38,50]. These are long-standing central topics in both theoretical and experimental ultracold atomic gas systems. While the Floquet engineering in the bosonic systems has also been gaining significant attention [2,51–56], the study of the time-averaged spectral function in their bosonic counterparts is significantly lacking, despite the substantial progress having been made in the fermionic counterparts. To characterize Floquet-engineered bosonic systems, it is crucial to establish a framework for analyzing excitation spectra that remains applicable over a wide range of driving frequencies, rather than being restricted to the high-frequency limit.

Unlike electronic systems, the ultracold bosons suffer the following fundamental difficulties: (1) Isolated nature of the cold atomic systems prevents the system from relaxing to the effective temperature determined by the external periodic drive, and often ends up in the infinitely high temperature state given by the incoherent superposition of the Floquet states (Floquet thermalization) [57–61], since there is no mechanism to damp the energy in isolated systems. This is in contrast to solid-state systems, which are inherently open systems that constantly exchange energy with other degrees of freedom, such as quasiparticles, temperature fluctuations, or impurities. (2) The lack of Pauli blocking forbids the use of the perturbative analysis near the Fermi energy. Of course, it would be possible to utilize the effective theory, such as Magnus's high-frequency expansion [1,2,17], to visualize the Floquet quasienergy and states. However, in which state the bosons are condensed is important in determining the Floquet excitation spectra of the many-boson systems, and this cannot be obtained from the simple Magnus expansion alone. More sophisticated and rigorous analysis is desirable to study the Floquet spectral function of the bosonic systems.

Here, we provide a rigorous study of the excitation spectra of the interacting bosonic systems in the Tonks-Girardeau (TG) limit [62] under a strong periodic drive. By the aid of the integrability of the system through the Bose-Fermi mapping theorem [62–66], the Floquet thermalization can be avoided, and the time-averaged spectral function of the many-body

*Contact author: hoshu.hiyane@oist.jp

Published by the American Physical Society under the terms of the Creative Commons Attribution 4.0 International license. Further distribution of this work must maintain attribution to the author(s) and the published article's title, journal citation, and DOI.

bosonic systems can be determined exactly. We uncover the emergence of two nonequilibrium Lieb excitations analogous to those in the equilibrium systems [39,40,63,67,68], if the initial phase of the periodic drive is appropriately chosen. The mode I corresponds to the Bogoliubov quasiparticles [39,40] while mode II corresponds to the dark soliton state [69], respectively. We trace the origin of these excitations to the emergence of a Floquet-Fermi sea (FFS) in the mapped fermionic system, where particle and hole occupations are distinctly separated in the Floquet spectra.

As we do not rely on an effective Hamiltonian approach, such as those derived from high-frequency expansions [70], an exact analysis of the Floquet spectral function across the entire frequency range is possible, including the low-frequency regime. We find that the nature of the nonequilibrium Lieb excitations and the spectrum of the mapped fermions alter dramatically across this range, with the linear spectrum extending into the high quasienergy regime, hybridizing with the states in the second Floquet-Brillouin zone (FBZ).

Given that the Lieb-Liniger model represents one of the most celebrated benchmarks in exactly solvable one-dimensional (1D) equilibrium bosons [38–40,71,72], the reemergence of the Lieb excitations in a periodically driven one-dimensional bosonic system is of fundamental importance for understanding the dynamical properties of the many-body bosonic physics [38,48], and represents a significant advancement in bridging integrable equilibrium physics [39,40,63,69] and Floquet nonequilibrium dynamics.

Methods. To obtain the spectral function of the periodically driven TG gas, we evaluate the lesser and greater Green's functions $G^{<,>}(t_1, t_2)$ exactly and efficiently by using the Bose-Fermi mapping theorem [62,63,73]. We rewrite these two-time Green's functions in Wigner coordinates, with relative time $t = t_1 - t_2$ and average time $t_{\rm avg} = (t_1 + t_2)/2$. A Fourier transform with respect to t gives the frequency-resolved Green's functions with frequency ω. In static systems, a continuous translational symmetry in $t_{\rm avg}$ reduces the $G^{<,>}(\omega)$ independent of $t_{\rm avg}$. In a periodically driven system, on the other hand, the remaining dependence on $t_{\rm avg}$ is periodic with the driving period and can therefore be decomposed into Floquet harmonics. Averaging over one period selects the zeroth Floquet component. The time-averaged spectral function is then defined as $\pi A_0(\omega) = -\mathrm{Im}[G_0^<(\omega) + G_0^>(\omega)]$, which is peaked at the Floquet quasienergy with peak height determined by occupation and transition matrix elements of the Floquet states. Further details are given in the Supplemental Material (SM) [73].

Model. We consider a TG gas confined in a hard-wall box potential and a deep optical lattice. At $t = t_0$, a time-dependent external potential with a static tilt, $w_n(t) = (V_0/2)\sin(\Omega t - \Phi n + \Phi/2) + \Omega n$, is applied to induce laser-assisted tunneling [1,5,6,74–77]. The Hamiltonian of the mapped fermions in the rotating frame can be written as [73]

$$\hat{H}(t) = -J\sum_{n=1}^{N_s-1} e^{-i\chi_n(t)\Theta(t-t_0)}\hat{a}_n^\dagger\hat{a}_{n+1} + \mathrm{H.c.}, \qquad (1)$$

where N_s is the number of lattice sites and $\hat{a}_n$ ($\hat{a}_n^\dagger$) represents the annihilation (creation) operator for a mapped fermion at site n. The time-dependent Peierls phase is given by

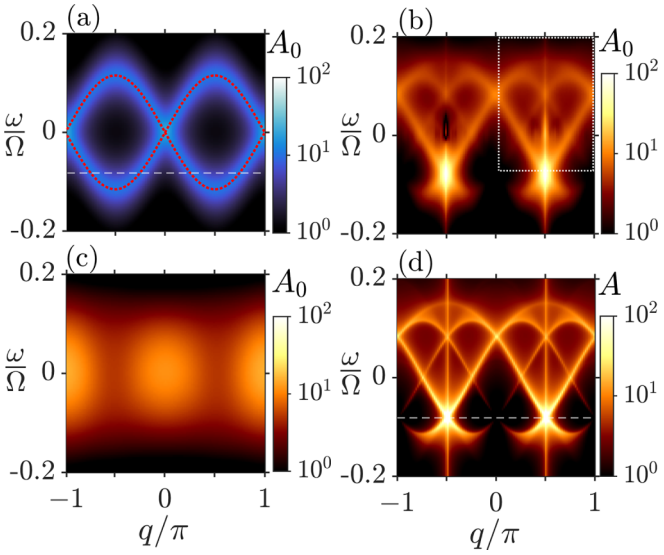


FIG. 1. Exact time-averaged spectral function of (a) mapped fermions and (b), (c) TG gas for two representative t_0. (d) Static spectral function of TG gas obtained from the effective Hamiltonian in Eq. (2). The periodic drive is applied at (a), (b) $t_0^{(1)} = -751.75T$ and (c) $t_0^{(2)} = -752T$. The rest of the parameter choices are $V_0 = 20J$, $\Omega = 10J$, $N_s = 120$, and $N = 30$ particles. The red dotted line in panel (a) shows the single-particle spectrum of mapped fermions in the effective Hamiltonian. The dashed line in panels (a) and (d) shows the Fermi energy of the effective Hamiltonian.

$\chi_n = -\int^t dt'[w_n(t') - w_{n+1}(t')] + \chi_n^0$, with χ_n^0 being a constant gauge term [2,78,79]. For high driving frequencies ($\Omega \gg 4J$), the effective time-averaged Hamiltonian $\hat{H}_{\rm eff}$ describes the systems quite well and is given by [1]

$$\hat{H}_{\rm eff} = -J\mathcal{J}_1(B)\sum_{n=1}^{N_s-1} e^{-i\Phi n}\hat{a}_n^\dagger\hat{a}_{n+1} + \mathrm{H.c.}, \qquad (2)$$

where $\mathcal{J}_1$ is the first-order Bessel function of the first kind and $B = (V_0/\Omega)\sin(\Phi/2)$. To benchmark our framework, we consider a 1/4-filled system with $\Phi = \pi$ in this paper, where the driving generates a Su-Schrieffer-Heeger-like two-band structure described by $E_{\rm eff}(k) = \pm 2J\mathcal{J}_1(B)|\sin(k)|$ [see Fig. 1(a)] [80,81].

Emergence of nonequilibrium Lieb modes. We start our discussion by focusing on the high-frequency regime ($\Omega = 10J$) with a strong drive ($V_0 = 20J$). The initial driving time t_0 is chosen to be significantly larger than the driving period ($|t_0| \gg T$). This condition ensures that initial transient effects do not affect the long-term dynamics. In the following, we discuss two representative values, $t_0^{(1)} = -751.75T$ and $t_0^{(2)} = -752T$, which illustrate the underlying physics within a single driving period, and the full t_0 dependence of the spectral function is discussed in the SM [73].

As can be seen from Fig. 1(a), the time-averaged spectral function of the mapped fermions is sharply peaked at the single-particle quasienergies, which are well reproduced by the effective Hamiltonian in the high-frequency limit. Due to the hopping term having a different value for alternating sites, a two-band structure emerges, and the Brillouin zone is reduced to $q \in [-\pi/2, \pi/2]$ [81].

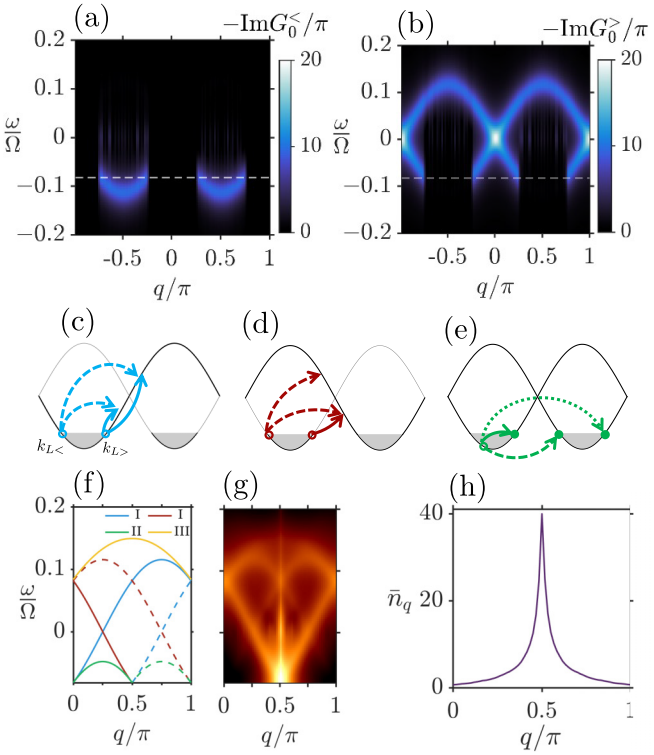


FIG. 2. The occupation of (a) mapped fermions and (b) holes visualized by the time-averaged imaginary part of the lesser and greater Green's function, respectively. Clear particle and hole separation is observed leading to a notion of Floquet-Fermi sea. The excitation processes (c) and (d) give rise to Lieb-I mode, while (e) to Lieb-II mode. The Fermi sea located within $k \in [k_{L<}, k_{L>}]$, where $(k_{L<}, k_{L>}) = (-3\pi/4, -\pi/4)$, is referred as the left Fermi sea, and the one within $k \in [\pi/4, 3\pi/4]$ as the right Fermi sea. Corresponding excitation spectra are depicted in panel (f) for the sector at the positive q and $\omega > E_{\mathrm{F}}^{\mathrm{eff}}$. (g) Cut along the white dotted region in Fig. 1(b). (h) Time-averaged momentum distribution. Here, the initial driving time is chosen at $t_0 = t_0^{(1)}$.

On the other hand, the excitation spectrum of the TG bosons is strongly influenced by many-body properties, which in the static systems results in the appearance of the Lieb modes [39,40,63,69]. Similar to the mapped fermions, we observe excellent agreement between the exact time-averaged spectral function A_0 and the static spectral function A for $t_0^{(1)}$ [see Figs. 1(b) and 1(d)]; however, unlike mapped fermions [73,82], these two differ significantly for $t_0^{(2)}$ [see Fig. 1(c)]. As we are in the Floquet regime, Figs. 1(b) and 1(c) should be interpreted as the Floquet spectral function of the TG gas, and the sharp peaks observed can be interpreted as Lieb excitations emerging in this nonequilibrium system. In the following, we elucidate the origin of these nonequilibrium Lieb modes and their strong dependence on t_0.

To understand the excitation spectrum of the driven TG bosons, it is helpful to consider the spectral distribution of the particles and holes, which can be visualized from the imaginary parts of the time-averaged lesser and greater Green's functions of the mapped fermions. In Figs. 2(a) and 2(b), we show them for $t_0^{(1)}$, where a clear separation between particle and hole occupations is visible. Therefore, we conclude that the excitation spectrum shown in Fig. 1(b) predominantly originates from excitation processes from a single Floquet-Fermi degenerate state, which we shall call the FFS state with many-body quasienergies E_{FFS}. Interestingly, this FFS is positioned below the Fermi energy of the effective Hamiltonian, which is interesting as there is no apparent mechanism to provide the ground state of the $\hat{H}_{\mathrm{eff}}$ in such isolated driven systems. Then, analogous to the static pure systems, the time-averaged greater Green's function for the TG gas possesses poles at excitation energies determined by $\omega = E_m - E_{\mathrm{FFS}} + \alpha\Omega$, where E_m is the Floquet quasienergy and $\alpha\Omega$ ($\alpha \in \mathbb{Z}$) implying the Floquet replica bands. The spectral weight is determined by both the occupations of the Floquet states, as specified by the FFS for $t_0 = t^{(1)}$, and the corresponding matrix elements.

Excitation from Floquet-Fermi sea. In the case of 1/4-filling and $\Phi = \pi$, considered in this study, two split Fermi seas exist, as indicated by the grey regions in Figs. 2(c)–2(e). To identify the Lieb-I mode, we analyze excitations from the left Fermi sea of the mapped Fermi gas to the branch $E_\pm \equiv \pm 2J\mathcal{J}_1(B)\sin(k)$, indicated with thick lines in Figs. 2(c) and 2(d), respectively. As shown by the solid arrows in Fig. 2(c), an excitation from a particle near $k_{L>}$ to the E_+ branch results in the gapless Lieb-I mode, depicted by solid lines of the same color (blue) in Fig. 2(f). Additionally, one can excite the particles from the opposite edge of the Fermi sea near $k_{L<}$ with the same excitation energies but different quasimomenta [dashed arrow in Fig. 2(c)], producing a branch shifted by $\pi/2$ in quasimomentum ($q \to q + \pi/2$) [dashed blue line in Fig. 2(f)]. Due to the two-band structure of the quasienergy spectrum, there also exist Lieb-I modes originating from excitations near $k_{L>}$ and $k_{L<}$ to the E_- branch, as described in Fig. 2(d), which create the Lieb-I mode depicted by the red lines in Fig. 2(f).

Additionally, the lowest many-body excitation branch for a given q is called the Lieb-II mode, and its excitation process is shown in Fig. 2(e). For instance, an excitation from the left Fermi sea to an unoccupied state near $k_{L>}$ produces this mode within the range of $q \in [0, \pi/2]$, resulting in the solid green line in Fig. 2(f). Furthermore, with the same excitation energy but shifted momentum ($q \to q + \pi/2$), one can also excite the Lieb-II mode to the right Fermi sea, resulting in the spectrum shown by the dashed green line in Fig. 2(f).

At sufficiently low energies, all particle-hole excitations are bounded by the Lieb-I and Lieb-II modes. For hard-core bosons in an optical lattice, however, the highest-energy excitation branch for a given q "bifurcates" from the Lieb-I mode at higher energies: The lower branch remains the Lieb-I mode, whereas an additional higher-energy branch emerges due to lattice effects [63]. The latter branch is indicated by the yellow line in Fig. 2(f).

The excitation spectra in the negative momentum regime ($q < 0$) can be constructed by considering excitation processes originating from the right Fermi sea. This results in a spectrum that is symmetric along $q = 0$, and the excitation spectrum is also symmetric with respect to $\omega \approx E_{\mathrm{F}}^{\mathrm{eff}}$ [83].

The time-averaged spectral function clearly captures the excitation spectrum with significant spectral weight concentrated around $q = \pi/2$ at $\omega \approx E_{\mathrm{F}}^{\mathrm{eff}}$ [Fig. 2(g)]. The time-averaged Floquet spectral function ($\ell = 0$) possesses

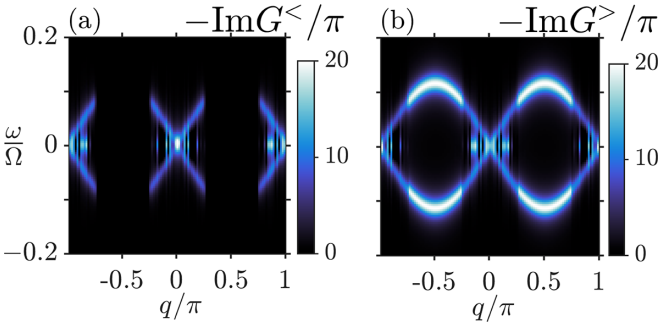


FIG. 3. The time-averaged (a) particle occupation and (b) hole occupation for $t_0 = t_0^{(2)}$.

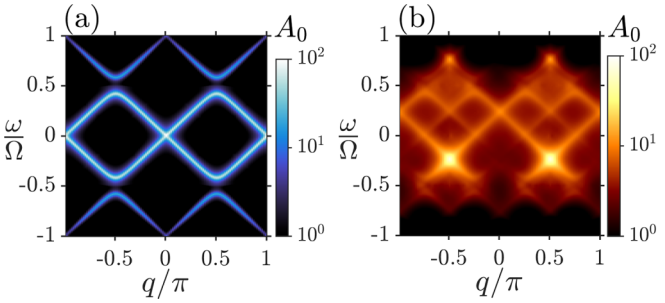


FIG. 4. Time-averaged spectral function of (a) mapped fermions and (b) TG bosons in the low-frequency regime with $\Omega = 2.5J$ and $V_0 = 5J$. The rest of the parameters are the same as in Fig. 1 with $t_0 = t_0^{(1)}$.

poles at the many-body excitation energies, weighted by the matrix element $|f_{mn}^{(0)}|^2$ of the many-body Floquet states. Although the direct visualization of such matrix elements is a difficult task, the spectral weight can be easily understood through the time-averaged momentum distribution [Fig. 2(h)]. The momentum distribution is calculated from the exact equal-time correlator, $iG^<(t,t)$ [84–87], which is related to the spectral function via [88]

$$n(q,t) = \frac{1}{2\pi i}\int_{-\infty}^{\infty} d\omega G^<(q,\omega,t_{\mathrm{avg}})|_{t_{\mathrm{avg}}=t}. \tag{3}$$

The clear Floquet-Fermi sea structure in the underlying mapped fermions leads to a time-averaged momentum distribution of the TG bosons that peaks at $q = \pm\pi/2$ and is strongly suppressed at $q = 0$, as can be seen from Fig. 2(h). Consequently, the spectral weight near $\omega = E_{\mathrm{F}}^{\mathrm{eff}}$ is predominantly concentrated around $q = \pm\pi/2$ and possesses negligible weight at $q = 0$.

Breakdown of Floquet-Fermi sea. At sufficiently long times $t \gg t_0$, which may be interpreted as $t_{\mathrm{avg}} \gg t_0$, one might expect that the initial time t_0 at which the periodic drive begins would no longer influence physical quantities. We show in Fig. 3 that this is indeed true for the spectral functions of the mapped fermions, where the particle and hole occupations complement each other, leading to a spectral function profile identical to Fig. 1(a) at the different t_0 (see Movies in SM for the full t_0 behavior [73]).

However, this is not the case for the TG bosons. Their time-averaged spectral function at $t_0^{(2)}$ [Fig. 1(c)] shows no resemblance to the result for $t_0^{(1)}$ [Fig. 1(b)] or the result from the effective Hamiltonian in Fig. 1(d). In particular, no sharp Lieb excitations are visible for $t_0^{(2)}$. This can be understood by realizing that the occupation of mapped fermions and holes are broad and overlap significantly (Fig. 3) and the occupation of the states is therefore composed of various Floquet states, and no FFS forms anymore. The excitations from such states produce the very broad spectrum seen in Fig. 1(c).

Exact analysis at low-frequency limit. As the driving frequency decreases, a higher-order Magnus expansion is required to accurately describe the system, with the nth order involving nested commutators of the form $[\hat{H}(t_1), [\hat{H}(t_2), \ldots, [\hat{H}(t_n), \hat{H}(t_{n+1})]\cdots]]$. Even if the exact Hamiltonian is noninteracting, the external periodic drive generates effective $(n+1)$-body interactions, making the analysis significantly more challenging [57–59]. However, as we compute the time-dependent spectral function exactly, we can rigorously analyze the systems in the low-frequency regime without the complexity inherent to the Magnus expansions at low frequency. As an example, we study the case of $\Omega = 2.5J$ and $V_0 = 5J$ in Fig. 4, for which the ratio Ω/V_0 is the same as for the values used in Fig. 1. Since the effective Hamiltonian in Eq. (2) is determined by the ratio Ω/V_0, the excitation spectrum obtained from the lowest Magnus expansion is the same as that in Fig. 1(a) (red dotted line) for mapped fermions and Fig. 1(d) for the TG gas.

One can immediately see that the time-averaged spectral function of the mapped fermions in Fig. 4(a) is in stark contrast to that in the fast-driving regime shown in Fig. 1(a). In this slow-driving case, the spectrum shows a characteristic linear behavior and extends nearly up to the edge of the Floquet-Brillouin zone. As a consequence, there exists a significant weight in the second FBZ, hybridizing with the first FBZ [89].

Due to this linearization of the mapped fermion's spectra, the linear regime of the nonequilibrium Lieb excitations is significantly extended over nearly the entire range of q in the first Brillouin zone [Fig. 4(b)]. Consequently, the Lieb-I mode hybridizes with its Floquet replica state in the second FBZ. These extended linear spectra suggest that a larger number of particles possess the same (phase) velocity, leading to the possibility of enhanced mobility. Such enhanced mobility may be of importance for applications in quantum technologies, leading to new devices with unique transport properties in atomtronics [90–92]. Further exploration of Floquet engineering in the low-frequency regime is therefore a promising direction for future research, since this regime's unique characteristics could yield new insights and applications in nonequilibrium quantum systems.

Conclusion. We have investigated the exact time-averaged spectral function of a gas of TG bosons under periodic driving, without relying on approximations based on an effective static Hamiltonian. We have demonstrated that nonequilibrium Lieb excitations emerge in the time-averaged spectral function of the TG gas if the initial phase of the driving pulse is chosen such that the underlying mapped fermions exhibit a Floquet-Fermi sea. Furthermore, our exact analysis in the low-frequency regime revealed the characteristic linear spectrum of Lieb excitations, emerging due to the effective many-body interaction mediated by the periodic drive. The

rigorous analysis presented here paves the way toward the spectral study of other bosonic systems, such as weakly correlated Bose-Einstein condensates, where the Bogoliubov/roton spectrum has been playing an important role in determining superfluid/supersolid properties in equilibrium systems. It is an important future work to extend the analysis developed here to Floquet-engineered bosonic superfluid/supersolid systems, which allow one to study their spectral properties. To this end, we remark two issues: (1) In such nonintegrable systems, the effect of the Floquet heating is non-negligible. This restricts the analysis to a finite driving time, limiting the frequency resolution. (2) As demonstrated here, even in the absence of Floquet heating, the excitation spectrum cannot in general be inferred solely from the effective high-frequency Hamiltonian, but depends significantly on the occupations of the Floquet states.

Acknowledgments. This work was supported by the Okinawa Institute of Science and Technology Graduate University. The authors are grateful to the Scientific Computing and Data Analysis (SCDA) section of the Research Support Division at OIST for their invaluable assistance. T.B. acknowledges additional support from the Japan Science and Technology Agency (JST) under Grant No. JPMJPF2221. S.W. thanks the support by JST, PRESTO Grant No. JPMJPR211A.

Data availability. The data that support the findings of this article are not publicly available upon publication because it is not technically feasible and/or the cost of preparing, depositing, and hosting the data would be prohibitive within the terms of this research project. The data are available from the authors upon reasonable request.

[1] M. Bukov and A. Polkovnikov, Stroboscopic versus nonstroboscopic dynamics in the Floquet realization of the Harper-Hofstadter Hamiltonian, Phys. Rev. A **90**, 043613 (2014).

[2] A. Eckardt, *Colloquium:* Atomic quantum gases in periodically driven optical lattices, Rev. Mod. Phys. **89**, 011004 (2017).

[3] T. Oka and S. Kitamura, Floquet engineering of quantum materials, Annu. Rev. Condens. Matter Phys. **10**, 387 (2019).

[4] C. Schweizer, F. Grusdt, M. Berngruber, L. Barbiero, E. Demler, N. Goldman, I. Bloch, and M. Aidelsburger, Floquet approach to $\mathbb{Z}_2$ lattice gauge theories with ultracold atoms in optical lattices, Nat. Phys. **15**, 1168 (2019).

[5] M. Aidelsburger, M. Atala, S. Nascimbène, S. Trotzky, Y.-A. Chen, and I. Bloch, Experimental realization of strong effective magnetic fields in an optical lattice, Phys. Rev. Lett. **107**, 255301 (2011).

[6] H. Miyake, G. A. Siviloglou, C. J. Kennedy, W. C. Burton, and W. Ketterle, Realizing the Harper Hamiltonian with laser-assisted tunneling in optical lattices, Phys. Rev. Lett. **111**, 185302 (2013).

[7] M. Atala, M. Aidelsburger, M. Lohse, J. T. Barreiro, B. Paredes, and I. Bloch, Observation of chiral currents with ultracold atoms in bosonic ladders, Nat. Phys. **10**, 588 (2014).

[8] M. Aidelsburger, M. Lohse, C. Schweizer, M. Atala, J. T. Barreiro, S. Nascimbène, N. R. Cooper, I. Bloch, and N. Goldman, Measuring the Chern number of Hofstadter bands with ultracold bosonic atoms, Nat. Phys. **11**, 162 (2015).

[9] M. Lohse, C. Schweizer, O. Zilberberg, M. Aidelsburger, and I. Bloch, A Thouless quantum pump with ultracold bosonic atoms in an optical superlattice, Nat. Phys. **12**, 350 (2016).

[10] C. Weitenberg and J. Simonet, Tailoring quantum gases by Floquet engineering, Nat. Phys. **17**, 1342 (2021).

[11] C. Monroe, D. M. Meekhof, B. E. King, W. M. Itano, and D. J. Wineland, Demonstration of a fundamental quantum logic gate, Phys. Rev. Lett. **75**, 4714 (1995).

[12] D. Leibfried, R. Blatt, C. Monroe, and D. Wineland, Quantum dynamics of single trapped ions, Rev. Mod. Phys. **75**, 281 (2003).

[13] D. Kielpinski, C. Monroe, and D. J. Wineland, Architecture for a large-scale ion-trap quantum computer, Nature (London) **417**, 709 (2002).

[14] C. D. Bruzewicz, J. Chiaverini, R. McConnell, and J. M. Sage, Trapped-ion quantum computing: Progress and challenges, Appl. Phys. Rev. **6**, 021314 (2019).

[15] A. F. Kemper, M. A. Sentef, B. Moritz, T. P. Devereaux, and J. K. Freericks, Review of the theoretical description of time-resolved angle-resolved photoemission spectroscopy in electron-phonon mediated superconductors, Ann. Phys. **529**, 1600235 (2017).

[16] N. Tsuji, Floquet states, in *Encyclopedia of Condensed Matter Physics*, 2nd ed., edited by T. Chakraborty (Academic Press, Oxford, 2024), pp. 967–980.

[17] M. Grifoni and P. Hänggi, Driven quantum tunneling, Phys. Rep. **304**, 229 (1998).

[18] M. Lenz, S. Wüster, C. J. Vale, N. R. Heckenberg, H. Rubinsztein-Dunlop, C. A. Holmes, G. J. Milburn, and M. J. Davis, Dynamical tunneling with ultracold atoms in magnetic microtraps, Phys. Rev. A **88**, 013635 (2013).

[19] J. K. Freericks, H. R. Krishnamurthy, and T. Pruschke, Theoretical description of time-resolved photoemission spectroscopy: Application to pump-probe experiments, Phys. Rev. Lett. **102**, 136401 (2009).

[20] M. Na, A. K. Mills, and D. J. Jones, Advancing time- and angle-resolved photoemission spectroscopy: The role of ultrafast laser development, Phys. Rep. **1036**, 1 (2023).

[21] F. Boschini, M. Zonno, and A. Damascelli, Time-resolved ARPES studies of quantum materials, Rev. Mod. Phys. **96**, 015003 (2024).

[22] F. Mahmood, C.-K. Chan, Z. Alpichshev, D. Gardner, Y. Lee, P. A. Lee, and N. Gedik, Selective scattering between Floquet–Bloch and Volkov states in a topological insulator, Nat. Phys. **12**, 306 (2016).

[23] C. Bao, P. Tang, D. Sun, and S. Zhou, Light-induced emergent phenomena in 2D materials and topological materials, Nat. Rev. Phys. **4**, 33 (2022).

[24] D. Choi, M. Mogi, U. De Giovannini, D. Azoury, B. Lv, Y. Su, H. Hübener, A. Rubio, and N. Gedik, Observation of Floquet–Bloch states in monolayer graphene, Nat. Phys. **21**, 1100 (2025).

[25] T. Oka and H. Aoki, Photovoltaic Hall effect in graphene, Phys. Rev. B **79**, 081406 (2009).

[26] T. Kitagawa, T. Oka, A. Brataas, L. Fu, and E. Demler, Transport properties of nonequilibrium systems under the application

of light: Photoinduced quantum Hall insulators without Landau levels, Phys. Rev. B **84**, 235108 (2011).
[27] J. Cayssol, B. Dóra, F. Simon, and R. Moessner, Floquet topological insulators, Phys. Status Solidi RRL **7**, 101 (2013).
[28] J. W. McIver, B. Schulte, F.-U. Stein, T. Matsuyama, G. Jotzu, G. Meier, and A. Cavalleri, Light-induced anomalous Hall effect in graphene, Nat. Phys. **16**, 38 (2020).
[29] M. S. Rudner and N. H. Lindner, Band structure engineering and non-equilibrium dynamics in Floquet topological insulators, Nat. Rev. Phys. **2**, 229 (2020).
[30] F. Chassot, A. Pulkkinen, G. Kremer, C. Wang, J. Schusser, J. Krempaský, J. Minár, G. Springholz, M. Puppin, J. H. Dil, and C. Monney, Floquet topological state induced by light-driven band inversion in SnTe, Nat. Phys. **22**, 1282 (2026).
[31] N. Li, U. Mehta, M. Lebrat, S. Gao, T. Kafle, R. Sapkota, H. C. Kapteyn, O. Granas, R. Nandkishore, and M. M. Murnane, Femtosecond modulation of electron correlations in a Luttinger liquid, Sci. Adv. **12**, eaec7494 (2026).
[32] T. Qin and W. Hofstetter, Spectral functions of a time-periodically driven Falicov-Kimball model: Real-space Floquet dynamical mean-field theory study, Phys. Rev. B **96**, 075134 (2017).
[33] A. Dutta, E. Sen, J.-H. Zheng, M. Aidelsburger, and W. Hofstetter, Anomalous Floquet Anderson insulator in a continuously driven optical lattice, Phys. Rev. B **109**, L121114 (2024).
[34] J.-H. Zheng, A. Dutta, M. Aidelsburger, and W. Hofstetter, Floquet topological phase transitions induced by uncorrelated or correlated disorder, Phys. Rev. B **109**, 184201 (2024).
[35] A. Schuckert, A. Bohrdt, E. Crane, and F. Grusdt, Visualizing spinon Fermi surfaces with time-dependent spectroscopy, Phys. Rev. B **104**, 235107 (2021).
[36] M. Aidelsburger, Artificial gauge fields and topology with ultracold atoms in optical lattices, J. Phys. B: At. Mol. Opt. Phys. **51**, 193001 (2018).
[37] K. Gadge and S. R. Manmana, Stability of Floquet sidebands and quantum coherence in one-dimensional strongly interacting spinless fermions, Phys. Rev. B **112**, 085144 (2025).
[38] L. Pitaevskii and S. Stringari, *Bose-Einstein Condensation and Superfluidity* (Oxford University Press, Oxford, UK, 2016), Vol. 164.
[39] E. H. Lieb and W. Liniger, Exact analysis of an interacting Bose gas. I. The general solution and the ground state, Phys. Rev. **130**, 1605 (1963).
[40] E. H. Lieb, Exact analysis of an interacting Bose gas. II. The excitation spectrum, Phys. Rev. **130**, 1616 (1963).
[41] M. R. Andrews, D. M. Kurn, H.-J. Miesner, D. S. Durfee, C. G. Townsend, S. Inouye, and W. Ketterle, Propagation of sound in a Bose-Einstein condensate, Phys. Rev. Lett. **79**, 553 (1997).
[42] R. Meppelink, S. B. Koller, and P. van der Straten, Sound propagation in a Bose-Einstein condensate at finite temperatures, Phys. Rev. A **80**, 043605 (2009).
[43] H. Hiyane, S. Watabe, and T. Nikuni, Collective excitations of a Bose-condensed gas: Fate of second sound in the crossover regime between hydrodynamic and collisionless regimes, Phys. Rev. A **109**, 033302 (2024).
[44] C. Barenghi and N. G. Parker, *A Primer on Quantum Fluids* (Springer International Publishing, Cham, Switzerland, 2016).
[45] K. E. Strecker, G. B. Partridge, A. G. Truscott, and R. G. Hulet, Formation and propagation of matter-wave soliton trains, Nature (London) **417**, 150 (2002).
[46] L. D. Carr and J. Brand, Spontaneous soliton formation and modulational instability in Bose-Einstein condensates, Phys. Rev. Lett. **92**, 040401 (2004).
[47] Y. Li, G. I. Martone, and S. Stringari, Spin-orbit-coupled Bose-Einstein condensates, in *Annual Review of Cold Atoms and Molecules* (World Scientific, Singapore, 2015), Vol. 3, pp. 201–250.
[48] G. Natale, R. M. W. van Bijnen, A. Patscheider, D. Petter, M. J. Mark, L. Chomaz, and F. Ferlaino, Excitation spectrum of a trapped dipolar supersolid and its experimental evidence, Phys. Rev. Lett. **123**, 050402 (2019).
[49] S.-C. Ji, L. Zhang, X.-T. Xu, Z. Wu, Y. Deng, S. Chen, and J.-W. Pan, Softening of roton and phonon modes in a Bose-Einstein condensate with spin-orbit coupling, Phys. Rev. Lett. **114**, 105301 (2015).
[50] D. De Santis, A. Gómez-Salvador, N. Bazhan, S. Erne, M. Prüfer, C. Guarcello, D. Valenti, J. Schmiedmayer, and E. Demler, Momentum-resolved two-dimensional spectroscopy as a probe of nonlinear quantum field dynamics, Phys. Rev. Lett. **136**, 233401 (2026).
[51] A. Eckardt, C. Weiss, and M. Holthaus, Superfluid-insulator transition in a periodically driven optical lattice, Phys. Rev. Lett. **95**, 260404 (2005).
[52] A. Schnell, L.-N. Wu, A. Widera, and A. Eckardt, Floquet-heating-induced Bose condensation in a scarlike mode of an open driven optical-lattice system, Phys. Rev. A **107**, L021301 (2023).
[53] Y. Zhang, Y. Chen, H. Lyu, and Y. Zhang, Quantum phases in spin-orbit-coupled Floquet spinor Bose gases, Phys. Rev. Res. **5**, 023160 (2023).
[54] C. Dauer, A. Pelster, and S. Eggert, Understanding Floquet resonances in ultracold quantum gas scattering, Phys. Rev. Lett. **135**, 033402 (2025).
[55] T. Wang, Y. Liu, J. Wang, Y. Huang, W. Chen, Z. Zhang, and J. Hu, Observation of modulation-induced Feshbach resonance, Phys. Rev. Lett. **135**, 203201 (2025).
[56] Y.-L. Pan, Q. Li, G.-P. Zheng, and Y. Zhang, Phase diagrams of spin-2 Floquet spinor Bose-Einstein condensates, Phys. Rev. A **113**, 033313 (2026).
[57] T. Mori, T. Kuwahara, and K. Saito, Rigorous bound on energy absorption and generic relaxation in periodically driven quantum systems, Phys. Rev. Lett. **116**, 120401 (2016).
[58] T. Kuwahara, T. Mori, and K. Saito, Floquet–Magnus theory and generic transient dynamics in periodically driven many-body quantum systems, Ann. Phys. **367**, 96 (2016).
[59] O. A. D. Sandberg, M. T. Reeves, and M. J. Davis, Floquet analysis of time-averaged trapping potentials, Phys. Rev. A **101**, 033615 (2020).
[60] D. A. Abanin, W. De Roeck, and F. Huveneers, Exponentially slow heating in periodically driven many-body systems, Phys. Rev. Lett. **115**, 256803 (2015).
[61] H. Olsen, P. Devillard, G. Aupetit-Diallo, P. Vignolo, and M. Albert, Interaction induced Anderson transition in a kicked

one dimensional Bose gas, Phys. Rev. Lett. **135**, 173403 (2025).
[62] M. Girardeau, Relationship between systems of impenetrable bosons and fermions in one dimension, J. Math. Phys. **1**, 516 (1960).
[63] J. Settino, N. Lo Gullo, F. Plastina, and A. Minguzzi, Exact spectral function of a Tonks–Girardeau gas in a lattice, Phys. Rev. Lett. **126**, 065301 (2021).
[64] Q.-W. Wang, Exact dynamical correlations of hard-core anyons in one-dimensional lattices, Phys. Rev. B **105**, 205143 (2022).
[65] O. I. Pâţu, A. Klümper, and A. Foerster, Exact spectral function and nonequilibrium dynamics of the strongly interacting Hubbard model, Phys. Rev. B **110**, 205101 (2024).
[66] W.-B. He, G. Žlabys, H. Hiyane, S. Sasidharan Nair, and T. Busch, Lieb excitations and topological flat mode of the spectral function of a Tonks-Girardeau gas in a Kronig-Penney potential Phys. Rev. A **111**, 013312 (2025).
[67] J.-S. Caux and P. Calabrese, Dynamical density-density correlations in the one-dimensional Bose gas, Phys. Rev. A **74**, 031605 (2006).
[68] S. Cheng, Y.-Y. Chen, X.-W. Guan, W.-L. Yang, R. Mondaini, and H.-Q. Lin, Exact spectral function of one-dimensional Bose gases, Natl. Sci. Rev. **12**, nwaf294 (2025).
[69] J. Sato, R. Kanamoto, E. Kaminishi, and T. Deguchi, Quantum states of dark solitons in the 1D Bose gas, New J. Phys. **18**, 075008 (2016).
[70] M. Bukov, L. D'Alessio, and A. Polkovnikov, Universal high-frequency behavior of periodically driven systems: From dynamical stabilization to Floquet engineering, Adv. Phys. (2015).
[71] T. Giamarchi, *Quantum Physics in One Dimension* (Oxford University Press, Oxford, UK, 2003).
[72] Y. Kuramoto and Y. Kato, *Dynamics of One-Dimensional Quantum Systems: Inverse-square Interaction Models* (Cambridge University Press, Cambridge, 2009).
[73] See Supplemental Material at http://link.aps.org/supplemental/10.1103/crbp-vdff for details of the fundamental theoretical framework, computational methods, and a movie illustrating the full dependence of the nonequilibrium spectral function on the initial phase.
[74] M. Aidelsburger, M. Atala, M. Lohse, J. T. Barreiro, B. Paredes, and I. Bloch, Realization of the Hofstadter Hamiltonian with ultracold atoms in optical lattices, Phys. Rev. Lett. **111**, 185301 (2013).
[75] N. Goldman, J. Dalibard, M. Aidelsburger, and N. R. Cooper, Periodically driven quantum matter: The case of resonant modulations, Phys. Rev. A **91**, 033632 (2015).
[76] R. Cruickshank, A. Di Carli, M. Mitchell, A. La Rooij, S. Kuhr, C. E. Creffield, and E. Haller, Phonon excitations of Floquet-driven superfluids in a tilted optical lattice, Phys. Rev. Res. **6**, 023323 (2024).
[77] A. Impertro, S. Huh, S. Karch, J. F. Wienand, I. Bloch, and M. Aidelsburger, Strongly interacting Meissner phases in large bosonic flux ladders, Nat. Phys. **21**, 895 (2025).
[78] A. Eckardt, P. Hauke, P. Soltan-Panahi, C. Becker, K. Sengstock, and M. Lewenstein, Frustrated quantum antiferromagnetism with ultracold bosons in a triangular lattice, Europhys. Lett. **89**, 10010 (2010).
[79] J. Struck, C. Ölschläger, M. Weinberg, P. Hauke, J. Simonet, A. Eckardt, M. Lewenstein, K. Sengstock, and P. Windpassinger, Tunable gauge potential for neutral and spinless particles in driven optical lattices, Phys. Rev. Lett. **108**, 225304 (2012).
[80] W. P. Su, J. R. Schrieffer, and A. J. Heeger, Solitons in polyacetylene, Phys. Rev. Lett. **42**, 1698 (1979).
[81] K. Lelas, N. Drpić, T. Dubček, D. Jukić, R. Pezer, and H. Buljan, Laser assisted tunneling in a Tonks–Girardeau gas, New J. Phys. **18**, 095002 (2016).
[82] G. S. Uhrig, M. H. Kalthoff, and J. K. Freericks, Positivity of the spectral densities of retarded Floquet Green functions, Phys. Rev. Lett. **122**, 130604 (2019).
[83] Note that the spectral weights for $\omega \lessgtr E_{\mathrm{F}}^{\mathrm{eff}}$ differ significantly, as can be seen from Fig. 1(b). This asymmetry arises because the sector of $\omega > E_{\mathrm{F}}^{\mathrm{eff}}$ corresponds to particle excitations governed by the propagator $G^{>}$, while $\omega < E_{\mathrm{F}}^{\mathrm{eff}}$ corresponds to hole excitations described by $G^{<}$. As there are more unoccupied states for Lieb-I (particle) excitations in the $\omega > E_{\mathrm{F}}^{\mathrm{eff}}$ region, this mode tends to dominate there. Conversely, the Lieb-II mode has a larger spectral weight in the $\omega < E_{\mathrm{F}}^{\mathrm{eff}}$ sector, as there are more unoccupied states for the hole excitation.
[84] R. Pezer and H. Buljan, Momentum distribution dynamics of a Tonks–Girardeau gas: Bragg reflections of a quantum many-body wave packet, Phys. Rev. Lett. **98**, 240403 (2007).
[85] P. Vignolo and A. Minguzzi, Universal contact for a Tonks-Girardeau gas at finite temperature, Phys. Rev. Lett. **110**, 020403 (2013).
[86] Y. Y. Atas, I. Bouchoule, D. M. Gangardt, and K. V. Kheruntsyan, Collective many-body bounce in the breathing-mode oscillations of a Tonks–Girardeau gas, Phys. Rev. A **96**, 041605 (2017).
[87] Y. Y. Atas, D. M. Gangardt, I. Bouchoule, and K. V. Kheruntsyan, Exact nonequilibrium dynamics of finite-temperature Tonks–Girardeau gases, Phys. Rev. A **95**, 043622 (2017).
[88] L. Kadanoff and G. Baym, *Quantum Statistical Mechanics: Green's Function Methods in Equilibrium and Nonequilibrium Problems*, Frontiers in Physics; A Lecture Note and Reprint Series (W. A. Benjamin, New York, NY, USA, 1962).
[89] While the occupation of the second Floquet-Brillouin zone is also visible in Figs. 1(a) and 1(b), it is significantly smaller than the weight in the first Floquet-Brillouin zone.
[90] L. Amico, D. Anderson, M. Boshier, J.-P. Brantut, L.-C. Kwek, A. Minguzzi, and W. von Klitzing, *Colloquium*: Atomtronic circuits: From many-body physics to quantum technologies, Rev. Mod. Phys. **94**, 041001 (2022).
[91] S. Jährling, V. P. Singh, and L. Mathey, Designing atomtronic circuits via superfluid dynamics Phys. Rev. Res. **7**, 033112 (2025).
[92] J. Polo, W. J. Chetcuti, E. C. Domanti, P. Kitson, A. Osterloh, F. Perciavalle, V. P. Singh, and L. Amico, Perspective on new implementations of atomtronic circuits, Quantum Sci. Technol. **9**, 030501 (2024).